

Constructing only the primary reflections in seismic data - without multiple removal

G.A. Meles, K. Wapenaar, A. Curtis and C. da Costa Filho

Summary

State of the art methods to image the Earth's subsurface using active-source seismic reflection data involve reverse-time migration (RTM). This, and other standard seismic processing methods such as velocity analysis, provide best results only when all waves in the data set are primaries (waves reflected only once). A variety of methods are therefore deployed as pre-processing to predict multiples (waves reflected several times); however, accurate removal of those predicted multiples from recorded data using adaptive subtraction techniques proves challenging, even in cases where they can be predicted with reasonable accuracy. We describe a new, alternative strategy: we construct a parallel data set consisting of only primaries, which is calculated directly from recorded data. This obviates the need for both multiple prediction and removal methods. Primaries are constructed using convolutional interferometry to combine first arriving events of up-going and direct-wave down-going Green's functions to virtual receivers in the subsurface. The required up-going wavefields to virtual receivers are constructed by Marchenko redatuming. Crucially, this is possible without detailed models of the Earth's subsurface velocity structure. The method is shown both to be particularly robust against errors in the reference velocity model used, and to improve migrated images substantially.

Introduction

Advanced seismic data processing methods such as full-waveform inversion can properly take into account data that includes multiply scattered waves. However, many current standard processing steps are based on the so-called Born approximation which states that waves have only scattered once from heterogeneities in the medium. This requires that data only include primaries (singly scattered waves) as multiples represent a source of coherent noise and must be suppressed to avoid artefacts. Multiples related to reflections from the Earth's free surface particularly impact on images resulting from seismic marine data, and much effort has been devoted to their removal (see review by Dragoset et al., 2010). By contrast, internal multiples affect both marine and land data, and relatively fewer techniques exist to predict and remove them from reflection data. We propose a new method to predict primaries directly, based on seismic interferometry and Marchenko redatuming; this substantially improves test images.

Theory

Seismic interferometry techniques synthesise Green's functions between source (or receiver) locations by integrating cross-correlations or convolutions of wavefields recorded by receivers (or emanating from sources) located elsewhere (Wapenaar and Fokkema, 2006). With these methods, one of the sources (or receivers) is essentially turned into a virtual receiver (or source). Marchenko redatuming on the other hand, estimates up- and down-going components of Green's functions between an arbitrary location in the Earth's subsurface where no sources (or receivers) are placed, and real receivers (or sources) located at the surface (Broggini et al., 2014). Similarly to standard linear migration methods, Marchenko focusing requires an estimate of the direct wave from the virtual source (or to the virtual receiver), illumination from only one side of the medium, and no physical sources (or receivers) inside the medium. We now show how these methods may be combined to predict internal multiples.

Convolutional interferometry uses acoustic reciprocity theorems to express the Green's function between two locations as (Wapenaar and Berkhout, 1989)

$$G(x_2, x_1) \approx \int_S \frac{2j\omega}{c(x)\rho(x)} \{G^-(x, x_2)G^+(x, x_1) - G^+(x, x_2)G^-(x, x_1)\} dS \quad (1)$$

where $c(x)$ indicates wave speed, and $G^{+/-}$ represent in/out-going Green's function components across closed surface S . The main contributions to interferometric surface integrals come from neighborhoods of points where the phase of the integrand is stationary (Snieder et al., 2006). Figure 1 illustrates how primary reflections are reconstructed in convolutional interferometry: equations (1) essentially pieces together and integrates up/down-going wavefields around each stationary point on horizontal sections of surface S , to calculate wavefields that would travel along each full wave path between x_1 and x_2 .

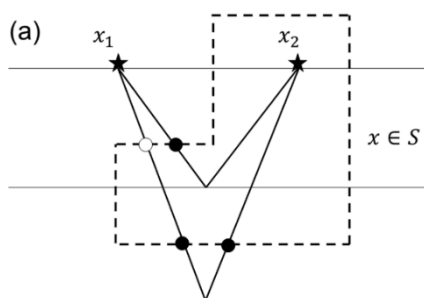


Figure 1 Geometrical configuration that constructs primaries from convolutional interferometry. Stars are sources at x_1 and x_2 , dashed line is an ideal receiver boundary S . (a) Circles indicate stationary points associated with primary reflections between x_1 and x_2 . Around each such point, convolutional interferometry connects a direct and a first-order scattering event to create a primary wave between x_1 and x_2 . Filled circles indicate stationary points x connecting direct waves $G_D^+(x, x_1)$ and the *first arriving* reflection in $G^-(x, x_2)$, or $G_D^+(x, x_2)$ and the *first arriving* reflection in $G^-(x, x_1)$. The unfilled circle indicates a stationary point x *not* connecting $G_D^+(x, x_1)$ and a first arriving reflection in $G^-(x_2, x)$.

Meles et al. (2015) noted that the number of reflections undergone by an event in $G(x_2, x_1)$ (its scattering order) is equal to the sum of the number of reflections undergone by its constitutive components, $G(x, x_1)$ and $G(x, x_2)$, and used that property to synthesize only multiple reflections. By contrast, in the

current paper we predict primaries directly, based on the observation that primaries may be constructed by convolving down-going direct waves with first-arriving up-going first-order scattered waves.

Following the standard decomposition of Green's functions into direct and scattered waves (e.g., $G(x, x') = G_D(x, x') + G_S(x, x')$, where $G_D(x, x')$ represents the component of $G(x, x')$ that does not undergo any reflection), direct waves are uniquely defined for any source-receiver pairs $G_D^+(x, x_1)$ or $G_D^+(x, x_2)$. By contrast, up-going Green's functions G_S^- comprise many first order scattering events (in addition to multiples). This is illustrated in Figure 1, which discriminates between the construction of two different primaries. Filled circles indicate points at which direct waves are pieced together with first-arriving events of scattered up-going Green's functions on surface S . The unfilled circle indicates a point where this does not apply: for that point the associated primary reflection $G_S^-(x, x_2)$ is not the *first* scattered arrival. Thus for *arbitrary* boundaries S , the components associated with primaries do not necessarily involve direct waves and first arriving events of up-going Green's functions.

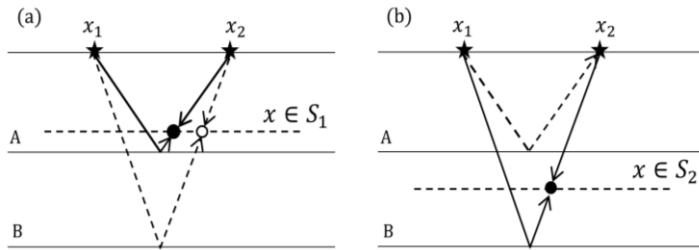


Figure 2 As Figure 1 but for horizontal truncated boundaries S_1 and S_2 . Solid rays: events involving direct waves and first arriving events of $G^-(x, x_1)$ which are reconstructed by equation 2. Dashed rays: events not involving first arriving events of $G^-(x, x_1)$.

In Figure 2 different partial boundaries (comprising only horizontal lines) are used to construct primaries. Filled circles and solid rays indicate points at which direct waves and first-arriving events of up-going Green's functions are pieced together at a stationary point to construct the corresponding primary. Unfilled circles and dashed rays indicate points at which a later-arriving singly-scattered event of the up-going Green's function must be used. Note that the reflection generated by reflector B is associated with later-arriving and first-arriving events in the up-going Green's functions when using boundaries S_1 and S_2 , respectively (Figure 2(a) and 2(b)). Keeping in mind the above observations and the limitations concerning performance of the method for different boundaries summarized in Figure 2, if we assume that the first arriving energy of any up-going Green's function $G^-(x_1, x)$ is associated with a singly-scattered event, then we can reconstruct primaries by combining such events with direct waves. More precisely, we postulate that primaries, and primaries only, are reconstructed when first-arriving up-going events are convolved with direct down-going Green's functions, and that for every primary there is always at least one surface on which this is true. We therefore propose the following approximate representation for primaries:

$$G_P(x_2, x_1) \approx \sum_i \int_{S_i} \frac{j\omega}{c(x)\rho(x)} \{G_F^-(x, x_2)G_D^+(x, x_1) + G_D^+(x, x_2)G_F^-(x, x_1)\} dS \quad (2)$$

where G_P stands for the primary arrivals in a Green's function, G_D^+ for the direct down-going wave, G_F^- for the first-arriving events of up-going components of Green's functions (which in our examples are created using Marchenko redatuming), and S_i is a partial (non-closed), horizontal boundary ($i=1,2,\dots$).

We distil this method into the following algorithm:

- 1) Choose a horizontal boundary S_i in the subsurface. Locate virtual receivers at regularly-sampled locations x along S_i , and use Marchenko redatuming to compute corresponding up-going Green's function $G^-(x, x_p)$, where source locations x_p span the surface array.
- 2) Mute events occurring before the direct waves in the up-going Green's functions $G^-(x, x_p)$ to remove possible Marchenko artefacts (Thorbecke et al., 2013).
- 3) Pick first-arriving event $G_F^-(x, x_p)$ in the muted up-going Green's function $G_M^-(x, x_p)$.
- 4) Apply equation 2 to predict primaries $G_P(x_j, x_k)$ for all x_j, x_k in the surface array.

- 5) Repeat steps 1 to 4 using S_i located at different depths to predict different primaries, then sum the results as specified in equation 2.

Numerical Example

We test the algorithm using a 2-dimensional varying density-velocity synclinal model (Figure 3). We compute synthetic surface seismic data with a finite-difference time domain modelling code and a

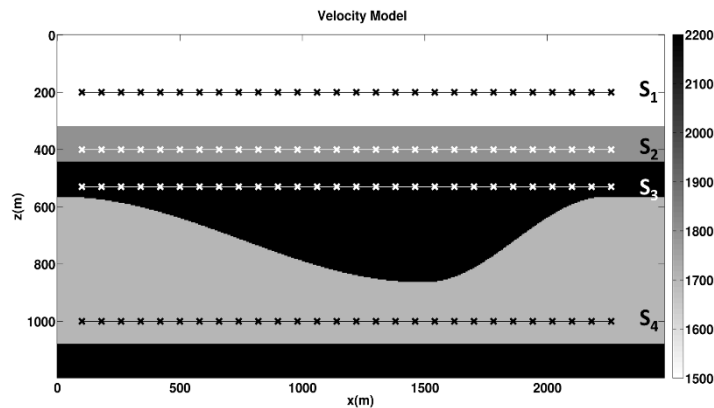
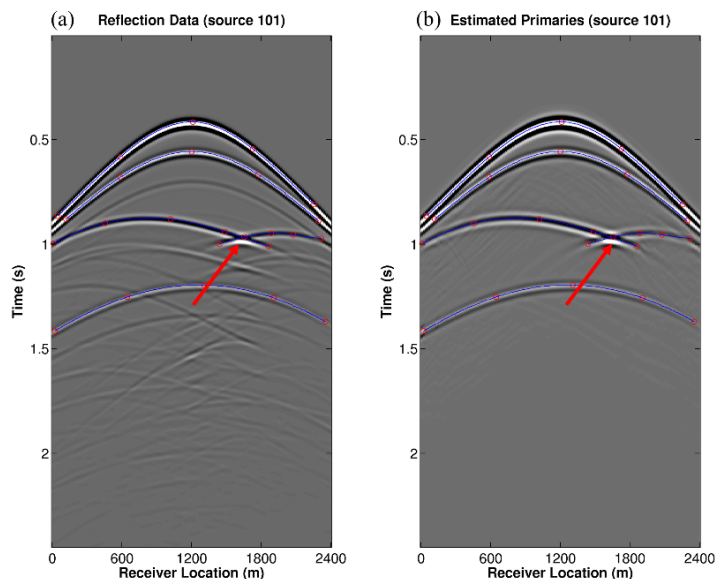


Figure 3 Velocity model used to compute reflection data. S_1 to S_4 represent surfaces used for integration in equation 2.



Ricker source wavelet with central frequency 20 Hz, using absorbing boundaries on all sides (thus assuming that surface-related multiples have been removed from recorded data), between 201 co-located sources and receivers equally spaced along the surface of the model shown in Figure 5, with inter-source spacing of 12 m. Partial boundaries consist of horizontal lines S_1 to S_4 in Figure 3. Up-going Green's functions $G^-(x, x_p)$ are estimated at a set of 121 points x along each boundary using Marchenko redatuming. We estimate direct waves $G_D^+(x, x_q)$ using a smooth velocity model. First arriving

Figure 4 (a) Observed reflection data for source 101, and (b) estimated primaries. The red arrows indicate two correctly synthesized events associated with a triplication from the synclinal interface. Each predicted primary corresponds to an actual primary reflection (indicated by blue curves in (a) and (b)). Low amplitude artefacts are due to inaccuracies in the picking process.

events of up-going Green's functions are then picked automatically and windowed. Despite inaccuracies in these wavefields and the consequent errors in picking, primaries, including the triplication associated with the synclinal interface, were relatively well reconstructed through application of equation 2, with only small, low amplitude artefacts (Figure 4). We then apply reverse time migration (RTM) to both the observed data and the estimated primaries using the smoothed reference velocity model. Resulting images are shown in Figure 5. Linear migration of internal multiples results in many multiple-related artefacts contaminating the conventional image (as indicated by red arrows in Figure 5(a)). RTM of only primaries provides a much cleaner image, with only a few artefacts below the top reflector (Figure 5(b)).

Conclusions

We present a new method to predict primary reflections based on Marchenko redatuming and convolutional interferometry. The method was demonstrated on acoustic data and proved to be stable with respect to inaccuracies in the redatumed Green's functions. The synthesized primaries were used

to produce images almost free of multiple-related artefacts via linear reverse-time migration. For simplicity, the method was tested on a dataset free of surface-related multiples, recorded for collocated sources and receivers. Extensions to datasets collected in standard acquisition setups and including ghosts and surface related multiples will be the topic of future research. Applications connected to other methods such as full-waveform inversion and velocity analysis will also be investigated.

Acknowledgments

We thank Matteo Ravasi for discussions that contributed to this paper. We are also grateful to the Edinburgh Interferometry Project (EIP) sponsors (ConocoPhillips, Schlumberger, Statoil and Total) for supporting this research.

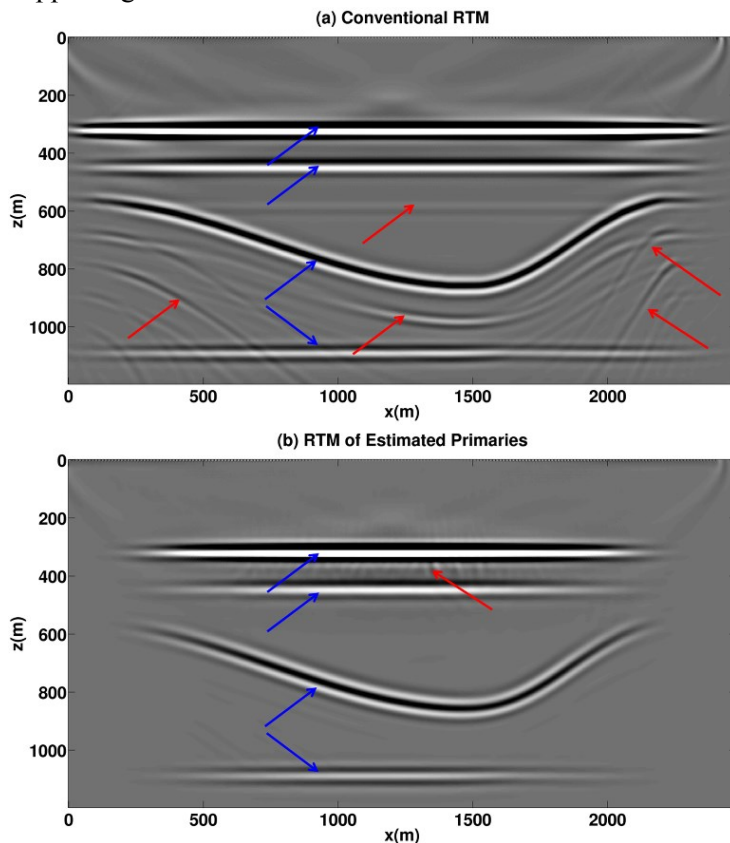


Figure 5 (a) RTM Image obtained by migrating the recorded data (primaries and internal multiples). Blue and red arrows indicate true reflectors and internal-multiple related artefacts, respectively. (b) RTM image obtained by migrating the primaries predicted by equation 2. Blue and red arrows indicate true reflectors and picking-related artefacts, respectively. Note that both images have saturated gray-scales at 25% of their maximum amplitude in order to highlight weaker, multiple-related artefacts.

References

Broggini, F., Snieder, R., and Wapenaar, K., 2014, Data-driven wave field focusing and imaging with multidimensional deconvolution: numerical examples for reflection data with internal multiples: *Geophysics*, Vol. 79 (3), WA107-WA115

Dragoset, B., Verschuur, E., Moore, I., and Bisley, R., 2010, A perspective on 3D surface-related multiple elimination, *Geophysics*, 2010, A245-A261.

Meles, G. L er, K., Ravasi, M., Curtis, A., da Costa Filho, C.A., 2015. Internal multiple prediction and removal using Marchenko autofocusing and seismic interferometry. *Geophysics* 80 (1), A7-A11.

Snieder, R., K. Wapenaar, and K. Larner, 2006, Spurious multiples in interferometric imaging of primaries: *Geophysics*, 71, no. 4, SI65–SI78.

Thorbecke, J., van der Neut, J., and Wapenaar, K., 2013, Green's function retrieval with Marchenko equations: a sensitivity analysis, 83rd annual SEG meeting, Houston, SPMI 6.3

Wapenaar, K. and Berkhout, A., 1989. *Elastic Wave Field Extrapolation: Redatuning of Single- and Multi-Component Seismic Data*, Elsevier Science Publ. Co., Inc.

Wapenaar, K., and Fokkema, J., 2006, Green's function representations for seismic interferometry: *Geophysics*, Vol. 71, SI33-SI46.